Differential effects of anti-Nogo-A antibody treatment and treadmill training in rats with incomplete spinal cord injury

Journal Article

Author(s):
Maier, Irin C.; Ichiyama, Ronaldo M.; Courtine, Grégoire; Schnell, Lisa; Lavrov, Igor; Edgerton, V. Reggie; Schwab, Martin E.

Publication date:
2009-06

Permanent link:
https://doi.org/10.3929/ethz-b-000019598

Originally published in:
Brain: A Journal of Neurology 132(6), https://doi.org/10.1093/brain/awp085

doi:10.1093/brain/awp085 Brain 2009: 132; 1426–1440 | 1426

BRAIN
A JOURNAL OF NEUROLOGY

Differential effects of anti-Nogo-A antibody treatment and treadmill training in rats with incomplete spinal cord injury

Irin C. Maier,[1,2,*] Ronaldo M. Ichiyama,[3,4,*] Grégoire Courtine,[4,5,*] Lisa Schnell,[1,2] Igor Lavrov,[4] V. Reggie Edgerton[4,6,7] and Martin E. Schwab[1,2]

1 Brain Research Institute, University of Zurich, Zurich, Switzerland
2 Department of Biology, Swiss Federal Institute of Technology, 8057 Zurich, Switzerland
3 Institute of Membrane and Systems Biology, University of Leeds, Leeds LS2 9JT, UK
4 Department of Physiological Science, University of California, Los Angeles, CA, USA
5 Experimental Neurorehabilitation Laboratory, University of Zurich, Zurich, Switzerland
6 Department of Neurobiology, University of California, Los Angeles, CA, USA
7 Brain Research Institute, University of California, Los Angeles, California 90095, USA

*These authors contributed equally to this work.

Correspondence to: Irin Maier,
Brain Research Institute,
Winterthurerstrasse 190,
8057 Zurich, Switzerland
E-mail: imaier@hifo.uzh.ch

Locomotor training on treadmills can improve recovery of stepping in spinal cord injured animals and patients. Likewise, lesioned rats treated with antibodies against the myelin associated neurite growth inhibitory protein, Nogo-A, showed increased regeneration, neuronal reorganization and behavioural improvements. A detailed kinematic analysis showed that the hindlimb kinematic patterns that developed in anti-Nogo-A antibody treated versus treadmill trained spinal cord injured rats were significantly different. The synchronous combined treatment group did not show synergistic effects. This lack of synergistic effects could not be explained by an increase in pain perception, sprouting of calcitonin gene-related peptide (CGRP) positive fibres or by interference of locomotor training with anti-Nogo-A antibody induced regeneration and sprouting of descending fibre tracts. The differential mechanisms leading to behavioural recovery during task-specific training and in regeneration or plasticity enhancing therapies have to be taken into account in designing combinatorial therapies so that their potential positive interactive effects can be fully expressed.

Keywords: spinal cord injury; locomotor training; Nogo-A; neuronal plasticity and regeneration; functional recovery

Abbreviations: BDA = biotindextrane amine; CGRP = calcitonin gene-related peptide; CNS = central nervous system; CST = corticospinal tract; PCA = principal component analysis; SCI = spinal cord injury

Introduction

There is growing awareness that optimal functional repair after spinal cord injuries (SCI) will require combined therapies to induce nerve fibre growth and regeneration, the formation of appropriate reconnections and optimal adaptation of regained or compensatory functions. A limited number of interventions are currently in clinical use or trials as a result of promising outcomes

Received September 25, 2008. Revised February 24, 2009. Accepted February 25, 2009. Advance Access publication April 16, 2009

in animal models. The benefits of locomotor training on the recovery of function after a spinal cord injury (SCI) have been demonstrated in animal models (Edgerton *et al*., 2004) and human patients (Barbeau and Rossignol, 1987; Dietz and Harkema, 2004). It is clear from those results that the spinal cord contains the necessary neuronal circuits to restore some locomotor ability even after a complete spinal cord transection (De Leon *et al*., 1998; Rossignol *et al*., 1999; Ichiyama *et al*., 2005). Step training after SCI induces plasticity in locomotor spinal circuits (Gomez-Pinilla *et al*., 2002; Tillakaratne *et al*., 2002; Petruska *et al*., 2007; Barriere *et al*., 2008), selectively reinforcing specific sensorimotor pathways (Ichiyama *et al*., 2008).

Because locomotor training and similar physiotherapeutical modalities are part of the treatment of SCI, the interaction with potential interventions aiming to promote axonal sprouting and regeneration are of urgent and critical clinical interest. Neurite growth inducing interventions in humans has not been used thus far. Studies in animal models have shown that an intrathecal infusion of antibodies or receptor fragments blocking the myelin associated neurite growth inhibitor Nogo-A leads to long distance regeneration of descending axons (Schwab, 2004; Liebscher *et al*., 2005; Harel and Strittmatter, 2006) and to an increase in compensatory fibre growth (Mullner *et al*., 2008). Fibre growth occurred at all levels of the spinal cord (Thallmair *et al*., 1998; Raineteau *et al*., 2001; Mullner *et al*., 2008) and was evident in different animal models, including primates (Liebscher *et al*., 2005; Freund *et al*., 2006). It was accompanied by behavioural improvements in sensorimotor functions and fine motor control in the absence of any obvious malfunction (Liebscher *et al*., 2005; Freund *et al*., 2006) suggesting that new fibres can establish appropriate functional connections.

The purpose of this study was to first study the detailed movement patterns that rats with partially injured spinal cords developed in response to anti-Nogo-A antibody (11C7) treatment or locomotor training. Secondly, we analysed the outcome of a combined, simultaneous treatment. Our results show clear behavioural recovery with both single treatments but with marked differences in hindlimb kinematic patterns after task-specific treadmill training versus anti-Nogo-A antibody treatment. Simultaneous application of both therapeutical interventions led to interference and inconsistent movement patterns.

Methods

Experimental setup

A total of 40 adult female Sprague-Dawley rats (200–250 g body weight) received the T-lesion, antibody treatment and locomotor training interventions described below. The entire experiment was repeated in a second set of 28 rats. There were no statistically significant differences in the outcome of lesions or behaviour between the two experiments, therefore, rats from the first ($n = 40$) and second ($n = 28$) experiment were pooled for behavioural analysis. Histological and morphological analyses were only performed on the second set of rats ($n = 28$). All procedures followed the National Institute of Health Guide for the Care and Use of Laboratory Animals and were approved by the Animal Use Committee at the University of California.

Surgical procedures

All surgical procedures were performed under aseptic conditions. Animals were deeply anaesthetized with an i.p. injection of a mixture of ketamine (100 mg/kg) and xylazine (10 mg/kg) and maintained at a deep level of anaesthesia with supplemental doses of ketamine as needed. Eye ointment was applied to protect the eyes from dehydration. A mid-dorsal incision was performed from approximately vertebral level C7 to L3, and the paravertebral muscles were reflected to expose the vertebral segment of interest. A laminectomy was performed at vertebral level T8 and the dura incised to expose the spinal cord. All animals received a T-shaped lesion (T8) previously described by Liebscher *et al*. (2005). In short, animals received a bilateral dorsal hemisection and a complete midline transection with small iridectomy scissors completely eliminating the dorsomedial, dorsolateral and ventromedial corticospinal tract components but sparing the ventral lateral funiculi.

Antibody treatment

Rats were randomly divided into two experimental groups: lesion + anti-Nogo-A antibody (11C7) treatment; and lesion + control mouse IgG treatment. The mouse monoclonal antibody 11C7 was raised against a peptide corresponding to the rat Nogo-A sequence amino acids 623–640 and has been described in detail (Oertle *et al*., 2003). Its Nogo-A function blocking capacity has been confirmed *in vitro* and *in vivo* (Liebscher *et al*., 2005; Weinmann *et al*., 2006; Mullner *et al*., 2008). A monoclonal mouse IgG directed against wheat auxin was used as control antibody. Because of potential autoimmune reactions, the use of antibodies against other myelin or CNS binding proteins as control proteins was avoided (Liebscher *et al*., 2005). After the spinal lesion was performed a small hole was drilled at vertebral level L2. A fine intrathecal catheter (32 gauge; Recathco, Allison Park, PA, USA) was inserted into the subdural space and carefully pushed up to T10. The catheter was anchored by suture to the paravertebral muscles and maintained at the lesion site. Antibodies were continuously delivered into the CSF from an osmotic minipump (5 µl/h, 3.1 µg IgG/µl, Alzet 2ML2; Charles River Laboratories, Les Oncins, France) for 2 weeks. Pumps and intrathecal catheters were removed after 2 weeks under isoflurane anesthesia. All experimenters were blind with regard to treatment throughout the experiment.

Locomotor training

In order to determine the severity of the lesion before the start of training, rats were tested in the open field BBB test (Basso *et al*., 1995) one week after injury and the variability between animals was small. Based on the combined scores for both legs, rats were divided into four counterbalanced groups (BBB scores 7 days after lesion were around 12 for all groups, see Supplementary Fig. 1). Anti-Nogo-A and control IgG antibody treated groups of each severity level were not significantly different from each other.

Locomotor training consisted of daily sessions (5 days/week) of 20 min bipedal treadmill training followed by 20 min quadrupedal treadmill training. Bipedal training has been used as a standard procedure in previous experiments after complete spinal cord transection (Edgerton *et al*., 2001). Due to the better locomotor performance after the incomplete transection additional

quadrupedal training at a high speed and on an incline plane was applied as an additional training paradigm to maximally challenge the animals during their training session. Training started 1 week post-injury and was carried out for 8 weeks. All individuals involved in handling and training of the rats were blind to the antibody groups.

For bipedal training, rats were placed in a servo-controlled body weight support (BWS) system (Timoszyk *et al*., 2005). A hollow cylinder made of heavy cloth was placed at the end of the BWS arm into which the rats freely placed their head and upper body, while their hindlimbs supported their weight on the moving treadmill belt. This procedure assured a bipedal stance, even though the rats were never stranded in a harness. Training started at 7 cm/s and reached a maximum of 21 cm/s for 20 min. In general, trained rats were able to step at 21 cm/s for 20 min by the third week of training.

Quadrupedal training immediately followed bipedal training and was performed on a dual lane treadmill, in which rats from both treatment groups were trained side-by-side. Similar to the bipedal protocol, training started at 7 cm/s and reached a maximum of 21 cm/s for 20 min.

In addition, the angle of inclination of the treadmill belt was systematically increased every week to reach a maximum 10% grade. Trained rats ran at an incline of 10% at 21 cm/s for 20 min by the fifth week of training. A sweet cereal reward was given to each rat after the bipedal and the quadrupedal training sessions.

Behavioural testing

Inclined climbing

To test the gain in locomotor function in response to both treatments all animals were tested on an additional completely novel motor task. Rats were not trained on the inclined climbing apparatus on a daily basis but acclimatized to the apparatus and testing conditions 1 week before testing.

During the acclimatization period each rat was placed on the apparatus and encouraged to climb all platforms, to the top of the apparatus. This procedure was repeated three times. The climbing apparatus is a new device engineered in the Edgerton laboratory. It consists of two rows of eight individual platforms staggered between left and right with an incline of 10°. The platforms are moveable and the distances between each platform can be manipulated between trials. The design allows intact rats to climb to the top of the apparatus by placing one paw on each individual platform at a time.

During testing, rats were placed at the base of the apparatus and encouraged to climb to the top, in three consecutive trials. The distances between platforms were randomly changed from the acclimatizing period. Cameras were placed perpendicular to the plane of climbing on either side of the apparatus and video images (60 frames/s) of each trial were captured.

Errors were counted by two independent observers, who were blind to the conditions. An error was counted when a rat failed to place the plantar surface of the hind paw on successive platforms during the climb. The following behaviours were observed and counted as errors: a platform was skipped; plantar placement but the paw slipped off the platform during push off; multiple attempts to plantar place on the same platform; or another part of the body contacted the platform.

Kinematic recording

Nine weeks after injury, all rats were tested on their ability to walk bipedally. Three-dimensional video recordings (100 Hz) were made using four cameras (Basler Vision Technologies, Ahrensburg, Germany) oriented at 45° and 135° with respect to the direction of the locomotion, i.e. the animal's sagittal plane, on both sides. Reflective markers were attached bilaterally to the shaved skin overlying specific bony landmarks: the greater trochanter (GT), the knee joint (K), the malleolus (M), the fifth metatarsal (MT) and the outside tip (T) of the fifth digit (Fig. 1). The SIMI motion capture software (SIMI Reality Motion Systems, Unterschleissheim, Germany) was used to obtain 3D coordinates of the markers. The body was modelled as an interconnected chain of rigid segments (Fig. 1), and the joint angles were generated accordingly. In particular, the limb axis was the segment connecting the iliac crest to the MT joint (toe). Classic step kinematics parameters, joint amplitudes and limb-axis motion were analysed from 10 to 15 consecutive steps (Courtine *et al*., 2008).

Data processing

Kinematics

Coordinates (x, y, z) of each marker were used to reconstruct the trajectory of the limb and to calculate joint angles at the hip, knee, ankle and fifth MT joints. The same convention as in non-human primates was used, i.e. flexion and the fifth MT plantar flexion were defined as a decrease in the measured angle (Courtine *et al*., 2005). A series of parameters describing the gait timing, the characteristics of limb end-point trajectory, and the spatial and temporal features of the kinematic patterns were measured for each animal as detailed below.

Gait timing

A gait cycle was defined as the time interval between two successive paw contacts of one limb. Successive paw contacts were visually defined by the investigators with an accuracy of ± 1 video frame. Ten successive, consistent hindlimb gait cycles were typically recorded from each animal. The onsets of the swing phases were set at the zero crossings of the rate of change of the elevation angle of the limb axis, i.e. at the onset of forward oscillation (Courtine *et al*., 2005). Cycle duration, and stance and swing durations were determined from the kinematic recordings. Footfall patterns were used to compute the coupling between the hindlimbs. In particular, the time at which the contralateral limb contacted the treadmill belt was expressed as a percent of the duration of the ipsilateral gait cycle. This parameter is typically 50% if both limbs move out of phase. In order to visualize step-to-step consistency and interlimb coordination, we plotted this parameter in a polar graph (Fig. 2a′–e′). In this representation, the angular value represents the phase coupling between the left and right limbs for a given cycle. Alternate, out of phase coordination between left and right hindlimb corresponds

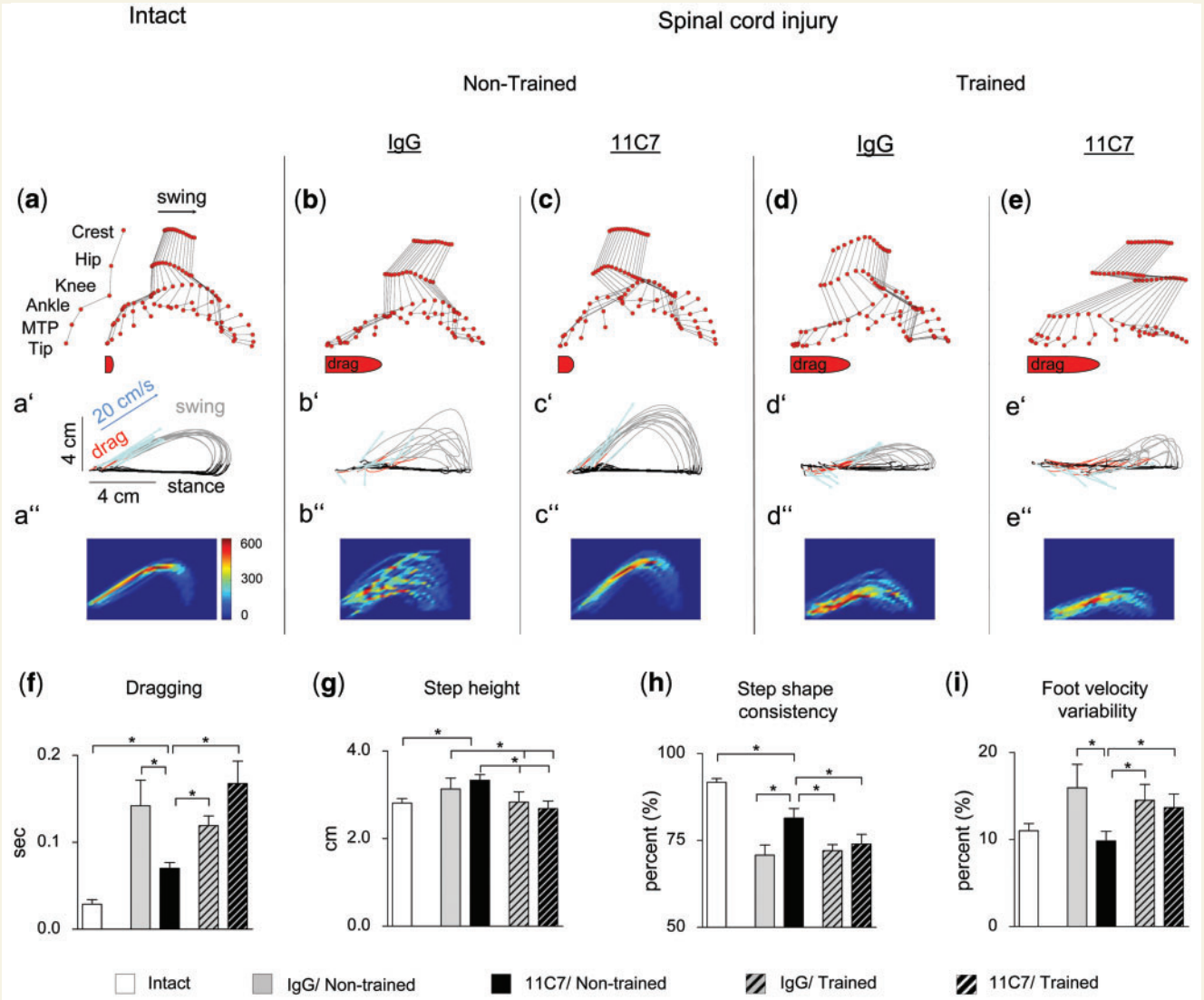

Figure 1 Kinematic analysis of hindlimb movements assessed during bipedal stepping. Representative stick diagrams of hindlimb movements during the swing phase of gait are shown for (**a**) intact (non-injured) as well as (**b**–**e**) injured animals nine weeks after injury in four different treatment groups (IgG or 11C7/non-trained, IgG or 11C7/trained). Segments run from iliac crest to proximal femur, knee, ankle, distal metatarsal phalange and end of the toe. The time between individual sticks is 30 ms. Successive trajectories of the hindlimb end-point during the stance (black) and swing (grey) phase are shown for 10 consecutive steps in (**a**′) intact (non-injured) as well as (**b**′–**e**′), injured animals nine weeks after injury in four different treatment groups (IgG or 11C7/non-trained, IgG or 11C7/trained). The periods of paw dragging are highlighted (red). Length and angle of blue arrows indicate the amplitude and orientation of limb acceleration at each swing onset, respectively. Spatial density of successive ($n = 10$ steps) trajectories of the hindlimb end-point illustrates variability between step cycles in (**a**″) intact and (**b**″–**e**″) injured animals in four treatment groups. Mean values of gait characteristics and hindlimb kinematics: (**f**) dragging, (**g**) step height, (**h**) step shape consistency and (**i**) foot velocity variability are shown for intact (non-injured) as well as injured animals of all treatment groups (IgG or 11C7/non-trained, IgG or 11C7/trained). Data are presented as means ± SEM. $^*P \leqslant 0.05$.

to a 180° value while the radius represents the duration of each step cycle to document cycle variability.

Limb end-point trajectory

In order to give insights into the control of foot motion, we analysed the trajectory of the MTP marker (MT), i.e. hindlimb end-point, relative to a fixed extrinsic frame attached to the treadmill. Stride length, linear path of end-point trajectory and step height were computed (Fong *et al.*, 2005).

Stance width was measured for each gait cycle as the perpendicular distance (medio-lateral plane) between left and right MT markers at the time of paw contact. The T-lesion of the spinal cord induced a dragging of the hind paws along the treadmill belt during stepping. The extent of the paw drag during each gait cycle was considered as the time during which the paw was in contact with the treadmill belt after swing onset.

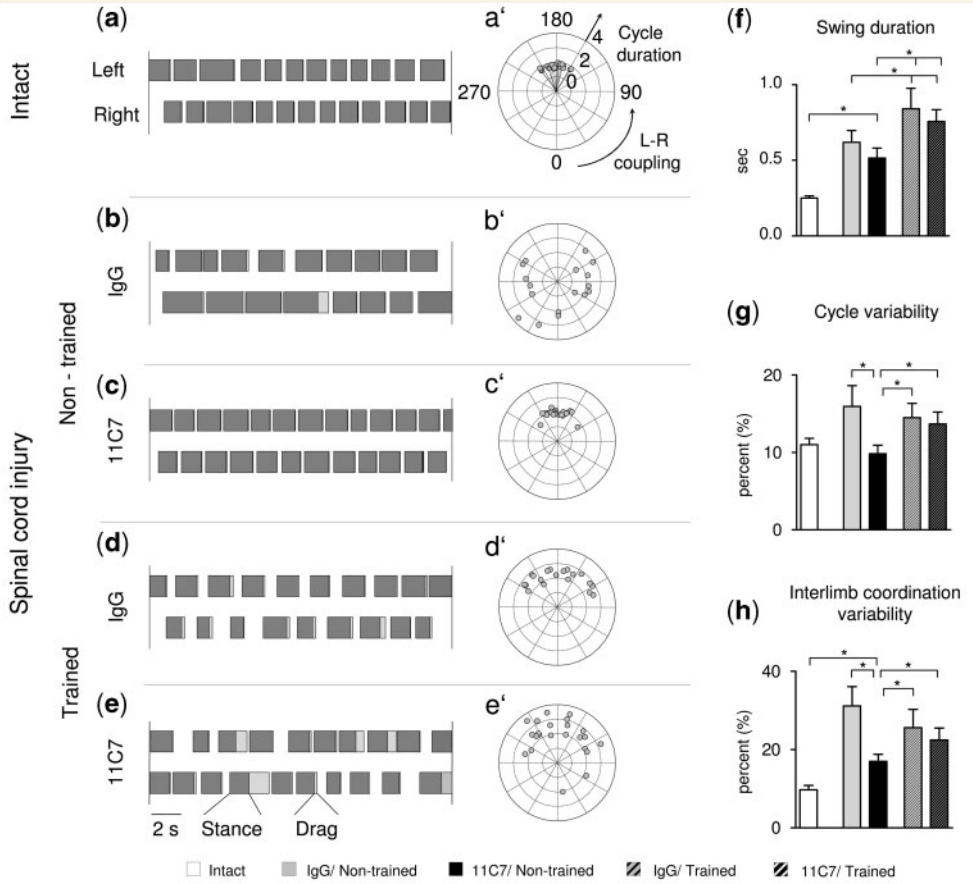

Figure 2 Coordination of hindlimb movements assessed during bipedal stepping. Footfall patterns are reconstructed at 7 cm/s and shown for (**a**) intact (non-injured) as well as (**b**–**e**), injured animals for each condition (IgG or 11C7/non-trained; IgG or 11C7/trained) 9 weeks after injury. Dark grey boxes with light grey endings represent the duration of stance and drag phases, empty spaces correspond to swing phases of gait, respectively. Each gait diagram represents 20 s of stepping. Values of interlimb coordination and cycle duration are represented in polar plots for (**a**′) intact (non-injured) as well as (**b**′–**e**′) injured animals for each treatment group (IgG or 11C7/non-trained; IgG or 11C7/trained). Each dot corresponds to one gait cycle extracted from the continuous sequence of stepping represented on the left aspect of each plot. The angular values represent the phase of left–right coupling for one gait cycle. Alternate, out-of-phase coordination between left and right hindlimb corresponds to a 180° value. The radius of each dot represents step cycle duration to document cycle variability. Mean values of gait characteristics and hindlimb kinematics: (**f**) swing duration, (**g**) cycle variablility and (**h**) interlimb coordination variability are shown for intact (non-injured) as well as injured animals of all treatment groups (IgG or 11C7/non-trained; IgG or 11C7/trained). Data are presented as means ± SEM. $*P \leqslant 0.05$.

To show the dynamics of foot motion during swing, we also calculated the instantaneous pitch angle of the hindlimb end-point velocity vector in the sagittal plane, i.e. the plane of walking trajectory. To assess the differences in the initial direction of hindlimb end-point motion at swing onset, we computed the mean pitch angle of MT velocity vector during the first 10% of swing.

We used principal component analysis (PCA) to quantify spatial consistency of hindlimb end-point trajectory as previously described (Fong *et al*., 2005). Spatial coordinates of hindlimb end-point trajectory were extracted from the selected sequence of stepping, and separated into their *x*, *y*, *z* components. For each gait cycle, each step component was resampled to 100 data points, thus removing the temporal information. The data were then arranged into three ($m \times n$) matrices, with each column containing the data for a single step and each row containing the interpolated position values at each time step. Matlab script was written to identify the principal components of each dataset and to calculate the PCA score. The PCA score reported here is the mean percentage of the total variance that is captured by the first principal component for each component. Hence, the higher the PCA score, the more consistent the stepping.

Coordination among joints

We used cross-correlation functions to assess coordination among joints of a single hindlimb. Cross-correlations among all unique pairs of degrees of freedom, i.e. hip, knee, ankle and MTP were calculated using the procedure detailed in Kubasak *et al*. (2008). The inter-joint R_{max} indicates the degree of correlation among a given pair of joints.

Joint angle shape

In order to compare the degree of similitude between joint angles produced by non-disabled versus experimental animals, typical templates for joint angles were obtained from kinematic patterns of a cohort of 24 non-disabled rats that stepped under the same conditions of posture and speeds as the experimental animals. Kinematic templates were computed by averaging time-normalized mean waveforms from each animal. Cross-correlation function was subsequently applied between non-disabled kinematic templates and mean time-normalized waveforms measured in a given experimental animal. The procedure was repeated for each animal, joint angle, and side. The highest positive correlation determined the degree of similitude between the actual waveform and the kinematic template obtained from non-disabled animals.

Variability of joint motion

To assess variability of joint angles across consecutive gait cycles, we computed SD of time normalized joint angles every 10% of the normalized time base. Variability of each joint angle was measured as the mean of SDs.

Dynamic features of joint motion

To evaluate joint motion frequency relative to non-disabled locomotion, the Frequency in Normal Range (FNR) was computed for each angle (Kubasak *et al*., 2008). The procedure consisted of identifying the frequency at peak power from Fast Fourier Transform of joint angles for each non-disabled animal ($n = 24$), and then constructing a band-pass filter centred at the mean FPP with a width of 2SDs. Subsequently, each joint angle from experimental animals was passed through the filter. The total signal energy within the frequencies typical of normal locomotion (FNR) was computed as the integral of the filtered FFT power spectrum over the entire range of frequencies. Mean joint angle speed was computed for each angle as the mean value of the angle joint velocity over the duration of the stepping period.

Principal component analysis

Performance of gait implies the rhythmic repetition of stereotypical patterns of leg motion. Several parameters need to be used in order to thoroughly characterize a given gait pattern, which can significantly complicate the extraction of relevant differences between experimental groups of animals. Nevertheless, both neural and biomechanical couplings result in strong co-variation between parameters that describe gait. Reduction of such multidimensional data sets can be achieved via multivariate statistical analysis such as PCA. PCA is mathematically defined as an orthogonal linear transformation that transforms the original data set to a new coordinate system such that the variance is maximized on each new coordinate axis. Data were analysed using the correlation method, which adjusts the mean of the data to zero and the SD to one. This is a conservative method and is appropriate for variables that differ in their variance. A set of 54 variables describing features of end-point trajectory, temporal characteristics of gait and spatiotemporal kinematic patterns of joint motions were submitted to PCA. PC was extracted, and a factor coordinate on each new PC axis computed (Courtine and Schieppati, 2004). The degree of similarities and differences between the animals were evaluated as differences in the respective factor coordinate on each principal component axis. In order to visualize differences between groups, we plotted coordinates from each animal in the new space created by the two fist PCs, which accounted for a large part of the variance (Fig. 4a). In this representation, the distance between the dots increases with the difference between the gaits of the animals.

Upon termination of locomotor training and completion of behavioural testing, all rats were shipped to the University of Zurich for further behavioural tests as well as histological and morphological analysis. All experiments were performed according to the guidelines of the Veterinary Office of the Canton of Zurich, Switzerland. All experimenters were blind with regard to treatment throughout the experiment.

Withdrawal reflex: Plantar Heater

Sensitivity of both hind paws to thermal heat stimulation was evaluated by performing a standardized Plantar Heater Test (Hargreaves *et al*., 1988) with an infrared source (Ugo Basile; Biological Research Apparatus, Comerio, Italy) producing a calibrated heating beam (diameter 1 mm). Each animal was placed in a small Plexiglas box ($9 \times 18 \times 8$ cm) on a thin Plexiglas floor (2.5 mm) and acclimatized to the testing conditions for 10 min followed by an initial trial. The reflex time for hindlimb withdrawal was then determined in four successive measurements for each hind paw. The average of all measurements was taken. Shortening of withdrawal latency indicated thermal hyperalgesia.

Tracing

Three weeks prior to perfusion, the animals were deeply anesthetized with a subcutaneous injection of Hypnorm (120 µl/200 g body weight; Janssen Pharmaceutics, Beerse, Belgium) and Dormicum (0.75 mg in 150 µl/200 g body weight; Roche Pharmaceuticals, Basel, Switzerland). A small hole was drilled into the skull 1 mm lateral and 1 mm posterior to bregma overlying the sensorimotor cortex. The CST was traced unilaterally with 10% biotin dextran amine (BDA, MW 10 000; Molecular Probes, Invitrogen, Carlsbad, CA) in 0.01 M phosphate buffered saline. We injected a total volume of 3.0 µl BDA at four sites of the sensorimotor cortex using a 5 µl Hamilton syringe. Analgesics (Rimadyl; 5 mg/kg, subcutaneous, Pfitzer AG, Zürich Switzerland) were given postoperatively.

Immunohistochemistry and histological analysis

Tissue preparation

Three weeks after BDA injections, the animals were deeply anaesthetized with pentobarbital (450 mg/kg i.p.; Abbott Laboratories, Cham, Switzerland), perfused transcardially with 100 ml Ringer's solution containing 100 000 IU/l heparin (Liquemin, Roche, Basel, Switzerland) and 0.25% $NaNO_2$ followed by 300 ml of 4% phosphate buffered paraformaldehyde, pH 7.4 containing 5% sucrose. Spinal cords and brains were dissected and

post-fixed in the same fixative over night at 4°C before they were cryoprotected in phosphate buffered 30% sucrose for an additional 5 days.

Quantification of corticospinal tract fibres

Brainstem and the thoracic spinal cord containing the lesion site as well as an area 1 cm rostral and 2 cm caudal of the lesion was embedded in Tissue tec OCT and frozen in isopentane at exactly −40°C. Parasagittal sections of 50 µm were cut on a cryostat and processed free floating using the nickel enhanced DAB protocol to show BDA tracing of corticospinal tract fibres as described previously (Herzog and Brosamle, 1997). Two days later all sections were dehydrated with alcohol and coverslipped with Eukitt (Kindler, Freiburg, Germany). Lesion size and extent were reconstructed for each animal from the sagittal section series and the extent of the lesion was determined as a percentage of spinal cord cross-section. Lesion size was reconstructed for each animal independently. There was little variability in lesion size between all groups; the lesion covered 40–50% of the cross sectional area of the spinal cord. Accordingly, there was little variability in BBB open field locomotor score between animals and rats were divided into four counterbalanced groups (BBB score around 12 for all groups one week after injury, Supplementary Fig. 1). Labelled CST fibres were counted in brightfield microscopy at a magnification of 400× as previously described (Liebscher *et al*., 2005). The number of CST fibres was evaluated in all sections lateral to the midline containing the traced corticospinal tract at four different regions (0.5, 2, 5 and 10 mm caudal to the lesion). To compensate for tracing variability the number of labelled CST fibres was determined on four adjacent cross sections in the main tract counted at the brainstem level.

Analysis of 5-HT and CGRP fibres

The lumbar spinal cord was embedded in Tissue tec OCT and frozen at –40°C in isopentane. Serial cross sections (50 µm) were obtained with a cryostat, collected as free-floating sections in 0.1 M phosphate buffered saline and prepared for immunohistochemistry. Staining as well as quantification of 5-HT (1:8000, rabbit, Immunostar) and calcitonin gene-related peptide (CGRP) (1:2000; rabbit, Immunostar) positive fibres was performed on alternating sections from lumbar level L3.

Staining for 5-HT was performed as previously described (Mullner *et al*., 2008); the same procedure was applied for the CGRP staining. Briefly, sections were stabilized by post-fixation (4% paraformaldehyde, 0.1% glutaraldehyde, 0.1% saturated picric acid in PB buffer) for 20 min, quenched with ethanol peroxide (50% ethanol plus 0.3% hydrogen peroxide in ddH_2O) and transferred into 0.2% sodium borohydride. Prior to microwave irradiation (twice at 600 W for 30 s) slides were incubated in citrate buffer ($M = 0.1$, pH = 4.5) over night at 4°C. The distribution of 5-HT and CGRP positive fibres was analysed in sections, and processed for immunoperoxidase DAB staining.

Quantification

A rectangular shape of 600 µm^2 was superimposed on Rexed's lamina VII on four alternate sections and on both, the left and right side of the spinal cord for each animal. 5-HT positive fibres were counted as previously described (Mullner *et al*., 2008). Fibre count was then divided by the surface area of the respective ventral horn to calculate the average relative fibre density (number of 5-HT positive fibre segments/mm^2) for each segment.

For quantification of 5-HT positive varicose appositions on lamina IX motoneurons six motoneurons were randomly chosen on each side of the cord on four consecutive sections for each animal (24 motoneurons/rat). 5-HT positive appositions were counted by criteria previously described (Mullner *et al*., 2008). The number of appositions was related to the cell body perimeter, which was measured with the AxioVision software, and expressed as number of 5-HT appositions per 100 µm cell surface.

Sprouting of CGRP positive fibres into the dorsal horn was evaluated in four adjacent sections. Images of the left and right dorsal horn were captured by a Zeiss AxioCam CCD camera and AxioVision software (Version 4.4, Zeiss, Jena, Germany). Images were analysed using the image analysing software ImageJ (a freely available image processing program). An outline was drawn on each picture around lamina I–IV and a second outline around the area occupied by CGRP positive fibres. CGRP sprouting was expressed in% area occupied by CGRP positive fibres within Rexeds lamina I–IV.

Statistics

Behavioural data were analysed using parametric analysis of variance (two-way ANOVA) for training and treatment effects with repeated measures for the left and right side followed by *post hoc* pair-wise comparisons whenever a main effect or interaction attained statistical significance. For histological and behavioural data presented in Figs 5 and 6, a non-parametric Mann–Whitney U-test was performed due to small animal numbers. Statistical analyses were conducted using the statistical software SPSS (release 14.0; Chicago, IL), Prism GraphPad or Statistica 8.0. Data are presented as means ± SEM, asterisks indicate significances: $*P \leqslant 0.05$, $**P \leqslant 0.01$.

Results

Locomotor impairments after incomplete spinal cord injury (Non-trained, control IgG treated animals)

The T-shaped lesion fully transected both dorsal funiculi, which include the main corticospinal tract (CST) and the ascending mechano- and proprioceptive fibres, as well as the dorso-lateral funiculi including the rubrospinal tract, and the ventral CST projections. The lesion only partially affected the reticulospinal or vestibulospinal tracts, classically associated with descending control

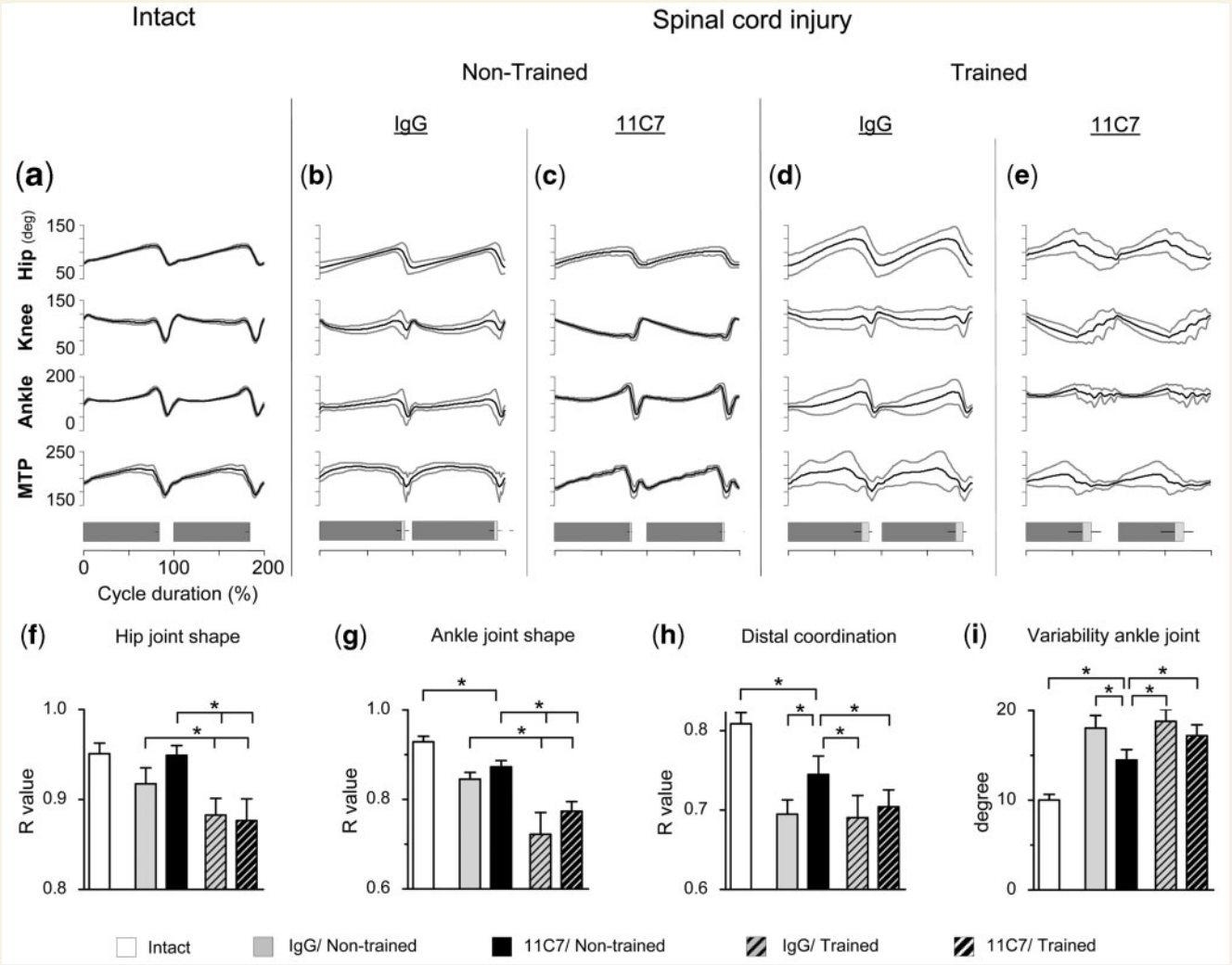

Figure 3 Mean (SD) waveforms of hip, knee, ankle and distal metatarsal phalange joint angle during bipedal treadmill locomotion in (**a**) non-injured as well as (**b–e**) injured animals 9 weeks after injury for each treatment group (IgG or 11C7/non-trained, IgG or 11C7/trained). Mean values of gait characteristics and hindlimb kinematics: (**f**) hip joint shape, (**g**) ankle joint shape, (**h**) distal coordination and (**i**) ankle joint variability are shown for intact (non-injured) as well as injured animals of all treatment groups (IgG or 11C7/non-trained, IgG or 11C7/trained). Data are presented as means ± SEM. $*P \leqslant 0.05$.

of locomotion (Freund *et al*., 2006). All rats were able to produce weight supported plantar stepping at least occasionally; BBB scores 7 days after lesion were around 12 for all groups (Supplementary Fig. 1). The injury resulted in quantifiable and significant changes in step kinematics as assessed during bipedal stepping at 9 weeks after injury (illustrated in Figs 1b–b″, f–i, 2b, b′, f–h and 3b, f–i; IgG/non-trained). Most notably, the T-lesion resulted in inconsistent step cycles (Figs 1b′, b″, 2b, b′ and g), a lack of left–right coordination (Fig. 2b, b′ and h), poor distal coordination (Fig. 3b and h) and pronounced dragging of the paws (Fig. 1b, f, 2b and 3b). The lesion also resulted in significant disturbance of all step kinematics parameters associated with spatio-temporal control, e.g. swing duration (Fig. 2b and f), step height (Fig. 1b′–b″ and g), hip joint shape (Fig. 3b and f), ankle joint shape (Fig. 1b and g) and movement consistency variables, e.g. step shape variability (Fig. 1b and h), joint angle variability (Fig. 3b and i), interlimb coordination variability (Fig. 2b and h) and foot velocity variability (Fig. 1i; IgG treated/non-trained).

Effect of anti-Nogo-A antibody treatment (11C7 treated, non-trained animals)

The effects of anti-Nogo-A antibody treatment on bipedal stepping are illustrated in Figs 1c–c″, f—i, 2c, c′, f–h, 3c, f–i (11C7 treated/non-trained). Without additional locomotor training, 11C7 treated rats at 9 weeks after injury demonstrated consistent step cycles (Figs 1c′, c″,2c, c′ and g) with good left right coordination (Fig. 2c, c′ and h), good distal coordination (Fig. 3c and h) and a very low level of paw drags (Figs 1c, f, 2c, 3c) when compared with all other groups 9 weeks after injury.

Accordingly 11C7 treated rats showed low variability in step shape (Fig. 1c and h), foot velocity (Fig. 1i) and ankle joint shape (Fig. 3c and i; 11C7 treated/non-trained). In all these parameters, anti-Nogo-A antibody treated animals approached the values of intact rats. Significant discrepancies, however, remained mainly with regard to a prolonged swing duration (Fig. 2c and f), changes in ankle joint shape (Fig. 3c and g) and an increased step height (Fig. 1c–c″ and g), which was partly due to a hyperflexion of knee and hip joints during swing. Rats also displayed some variability in step shape (Fig. 1c′, c″ and h), interlimb coordination, (Fig. 2c, c′ and h) distal coordination (Fig. 3c and h) and ankle joint shape (Fig. 3c and i).

In summary, stepping of non-trained anti-Nogo-A antibody treated animals on the treadmill was consistent, but hypermetric with short, well-coordinated steps, small variability and minimal toe dragging. The movement pattern of this animal group was closest to that of intact rats from all four treatment groups.

Effect of treadmill training (control IgG treated, trained animals)

The effects of treadmill training on bipedal stepping are illustrated in Figs 1d–d″, f–i, 2d, d′, f–h and 3d, f–i (IgG treated/trained). T-lesioned, trained rats showed slightly higher step cycle consistency (Figs 1d′, d″, 2d, d′ and g), and left–right coordination (Fig. 2d, d′ and h) than IgG treated, non-trained rats, but poor distal coordination (Fig. 3b and h) and pronounced dragging of the paws (Figs 1d, f, 2d and 3d). In contrast to non-injured control animals as well as untrained, 11C7 treated animals they showed high variability of step shape (Fig. 1d′–d″ and h), foot velocity (Fig. 1i) and ankle joint shape (Fig. 3d and i). These results show that the step pattern of treadmill trained animals was significantly different from both lesioned, untrained groups irrespective of antibody treatment. This was also reflected by their PCA scores (Fig. 4a and b). PCA analysis provides an overall measure for similarity and difference between animals based on a combination of detailed kinematics' parameters (see Methods section). Changes included a lower step height (Fig. 1d′–d″ and g) a greater swing duration (Fig. 2d and f) as well as a significantly different hip joint (Fig. 3d and f) and ankle joint shape (Fig. 3d and g).

In summary, step kinematics of treadmill trained spinal cord injured rats showed well coordinated, long but low steps with a high amount of variability and pronounced toe dragging.

Combined 11C7 administration and locomotor training (11C7 treated, trained animals)

Anti-Nogo-A antibody treatment by intrathecal pumps was started at the time of the lesion and lasted for 2 weeks. The rats started treadmill training seven days after the lesion, thus overlapping and extending beyond (for 7 weeks) the antibody application. The results of bipedal treadmill stepping are shown in Figs 1e–e″, f–i, 2e–e′, f–h and 3e, f–i (11C7 treated/trained).

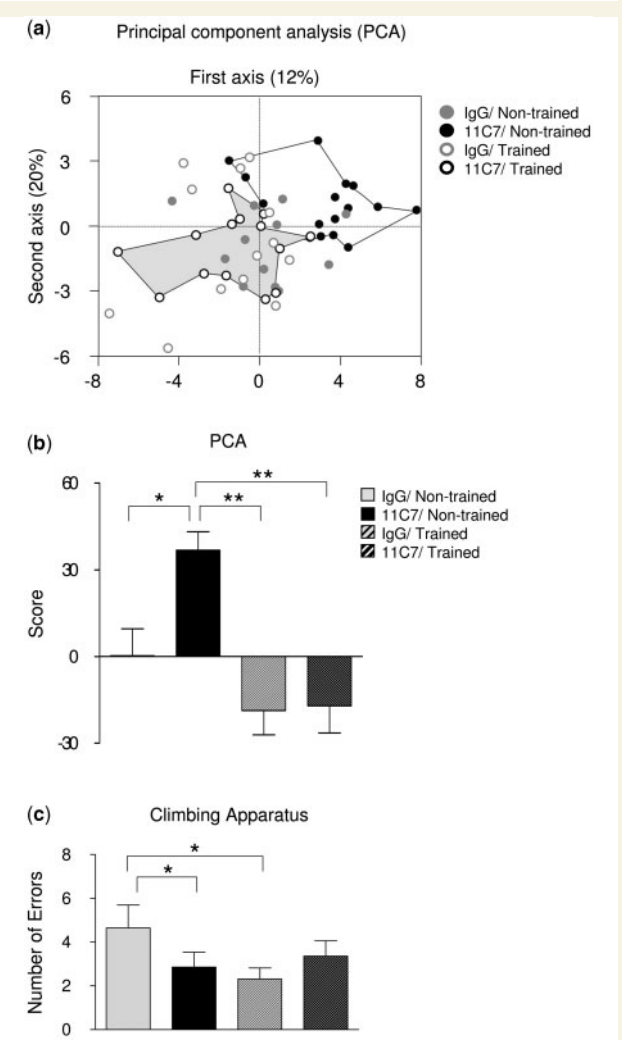

Figure 4 Analysis of detailed kinematics parameters. The degree of similarities and differences between groups is demonstrated by a multivariate statistical analysis applied on a large ($n = 54$) set of variables detailing gait performance. (**a**) Each dot corresponds to a single animal and was represented in space, defined by the two first PCs, which accounted for a large proportion of the total variance (32%). The spatial distance between each data point represents the degree of difference between gaits. Spatial space defined by the single data points are shown for two groups, 11C7 treated/untrained animals (white) and 11C7 treated/trained animals (grey). The near-absence of intersection revealed dramatic differences between the patterns of locomotion underlying treadmill stepping for these two groups of animals. (**b**) The scores on the first PC quantify (20% of explained variance) reveal critical differences between groups in their locomotor performance. Training (after IgG or 11C7 treatment) resulted in significant changes in intra- and interlimb step kinematics in comparison to non-trained/11C7 treated animals (ANOVA, $P \leqslant 0.01$). Locomotor performance on the inclined climbing apparatus. (**c**) Training alone and anti-Nogo-A antibody treatment alone resulted in significantly better performance on the climbing apparatus in comparison to IgG treated/non-trained animals (ANOVA, $P \leqslant 0.05$). Simultaneous application of anti-Nogo-A antibodies and locomotor training did not lead to synergistic effects ($P \leqslant 0.05$). Data are presented as means ± SEM. $^{*}P \leqslant 0.05$, $^{**}P \leqslant 0.01$.

These animals displayed low step shape consistency (Fig. 1c and h), and high variability of foot velocity (Fig. 1i) step cycle (Fig. 1e′, e″ and g), interlimb coordination (Fig. 2e, e′ and h) and ankle joint shape (Fig. 3e and i) as well as poor distal coordination (Fig. 3e and h) followed by a significant increase in paw dragging (Figs 1e, e′, f, 2e and 3e). The animals were similar to IgG treated, trained animals for many parameters, but significant differences between 11C7 treated, non-trained and 11C7 treated, trained animals emerged from PC analysis (Fig. 4b). The near-absence of intersection in the space defined by the data points from each group reveals dramatic differences between the patterns of locomotion during treadmill stepping for these two groups of animals (Fig. 4a).

Performance on the modified inclined grid walk

To further test the gain in locomotor function and the animals' ability to adapt their different movement strategies to locomotor challenges, they were tested on a completely novel, demanding motor task, the modified inclined plane. Both training alone and 11C7 treatment alone, resulted in significantly better performance, with fewer overall errors than non-trained, control IgG antibody treated animals (two-way ANOVA, Duncan's *post hoc*, $P \leqslant 0.05$). The simultaneous application of anti-Nogo-A antibodies and treadmill training did not result in further improvement.

Heat induced paw withdrawal test

To investigate a potential role of hyperalgesia on differences in behavioural recovery, animals were tested in their ability to respond to a simple heat stimulus applied to the sole of the hindlimb (Plantar Heater). Shortening of the withdrawal latency indicates thermal hyperalgesia, which could be associated with aberrant growth of nociceptive afferent fibres (Christensen and Hulsebosch 1997*b*; Ondarza *et al*., 2003). Animals were tested after locomotor training had been completed (9 weeks after injury). Rats of all groups responded to the heat stimulus by withdrawing their hind paws with a latency of 7.5 ± 0.15 s. No significant differences could be observed between the groups (Fig. 5e; Mann–Whitney U-test, $P > 0.05$), and this response latency did not differ from the reflex latency of uninjured animals (Liebscher *et al*., 2005). Thus, there was no indication of hyperalgesia in any of the groups that could explain differences in behavioural performance.

Nociceptive afferent fibre growth

CGRP is a neuropeptide enriched in nociceptive primary afferent fibres. To study if aberrant sprouting of afferent fibres could play a role in the behavioural recovery observed, CGRP positive fibres were stained in the lumbar spinal cord. All animals displayed strong CGRP immunoreactivity and dense fibres were typically visible throughout laminae I and II. CGRP positive fibres were absent in deeper laminae of the dorsal horn in all the treatment groups (Fig. 5a–d), a situation identical to that of the intact spinal cord. The proportion of the area of layers I–IV occupied by CGRP positive fibres was determined for each group. CGRP-positive axons occupied about 30% of the dorsal horn area and there were no significant differences between any of the groups (Fig. 5f; Mann–Whitney U-test, $P > 0.05$). Misdirected sprouting of nociceptive small diameter axons in the dorsal horn is, therefore, not a mechanism that could account for any of the behavioural effects observed.

Regeneration and sprouting of descending corticospinal tract fibres

Rats received a T-shaped lesion at T8, eliminating the CST as well as its minor dorso-lateral and ventro-medial components. In response to this injury, CST fibre retraction and the formation of retraction bulbs rostral to the lesion could be observed in all animals. In a few rats, very rare unlesioned fibres could be discriminated by their straight, regular appearance; these fibres were excluded from the analysis. In contrast to intact fibres, regenerating fibres were often fine and followed an irregular course around the lesion and scar tissue. They often grew outside of the original main CST territories with a considerable number of sprouts especially caudal to the lesion. Regenerating fibres were quantified on sagittal sections on four levels: at 0.5, 2.0, 5.0 and 10.0 mm caudal to the lesion. In both trained and non-trained control IgG groups, CST fibres in the caudal spinal cord were found only very rarely. The number of CST fibres was higher in the two 11C7 groups (Fig. 5m) with a significant increase after training (Mann–Whitney U-test, $P = 0.02$ for IgG/non-trained, $P = 0.006$ IgG/trained). Fine fibres with a thin axon caliber growing around the lesion, often on tissue bridges of the latero-ventral funiculi, were rare in the IgG groups (Fig. 5g and h) but frequently observed in both non-trained and trained 11C7 groups (Fig. 5i and j). BDA labelled CST fibres were also found caudal to the injury site in the 11C7 but not in the IgG treated groups (Fig. 5k and l). These results suggest that locomotor training alone could not increase sprouting and regeneration of descending CST fibres. Furthermore training did not enhance or interfere with the regenerative growth capacity of CST fibres after anti-Nogo-A antibody treatment.

Sprouting of serotonergic fibres in Rexed lamina VII

Serotonergic (5-HT) raphespinal tracts descend in the medial parts of the lateral and ventral funiculi and are in large parts but not completely transected after a T-shaped lesion (Mullner *et al*., 2008). In order to investigate a possible interference of locomotor training with regrowth of 5-HT fibres after anti-Nogo-A antibody treatment, the density of 5-HT fibres was quantified for the functionally important motor interneuron layer VII (Fig. 6a–e). Non-trained control IgG animals had low 5-HT fibre density in lamina VII of the lumbar spinal cord (Fig. 6a). 11C7 treatment significantly increased 5-HT fibre density in non-trained (Fig. 6c, $P = 0.006$) and trained animals (Fig. 6d, $P = 0.01$). Thus, for 5-HT fibres we observed a significant effect of anti-Nogo-A antibody treatment on 5-HT fibre density in lamina VII. Training did not

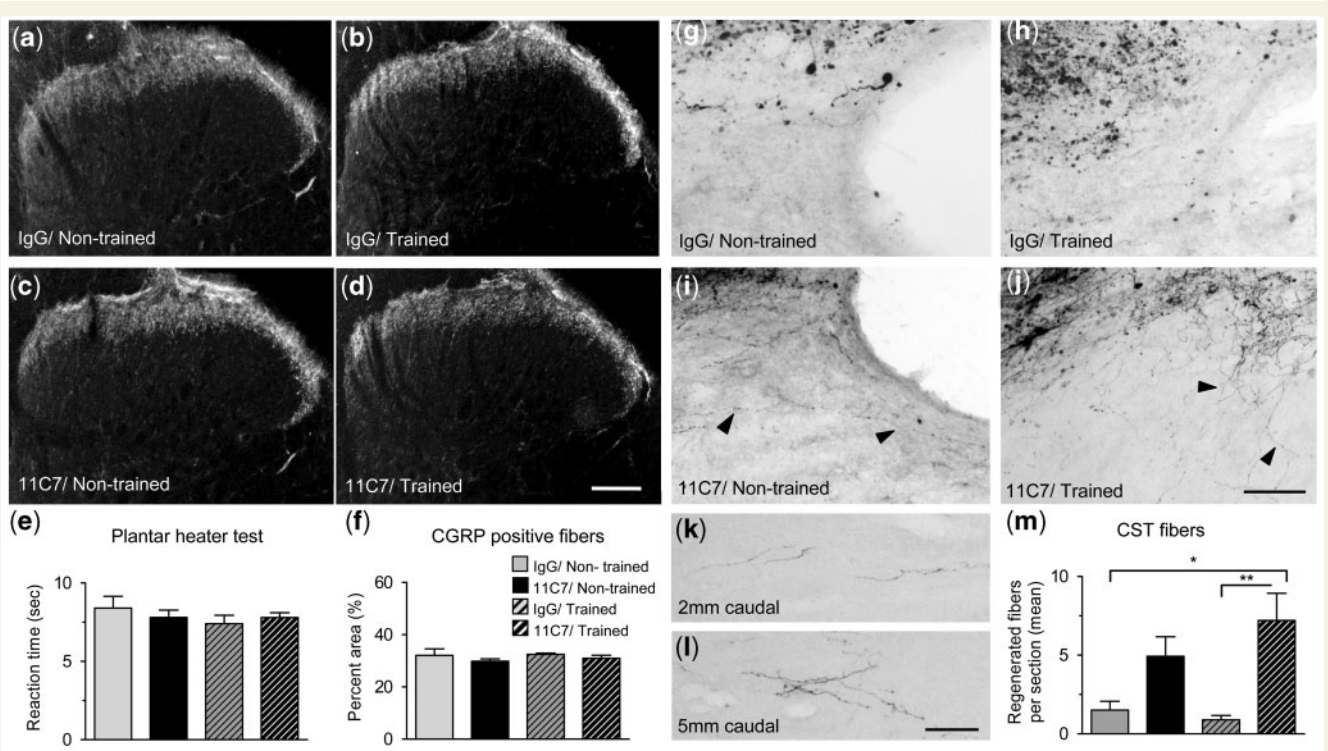

Figure 5 Localization of small diameter CGRP-positive pain fibres in the dorsal horn. Transverse sections of L3 spinal cord stained immunohistochemically for CGRP are shown for the four treatment groups. (**a**) Control IgG treated, non-trained; (**b**) IgG treated, trained; (**c**) 11C7 treated, non-trained and (**d**) 11C7, trained animals. All animals displayed dense CGRP immunoreactivity in laminae I and II and a near complete absence of CGRP-positive axons in the deeper laminae of the dorsal horn. (**f**) Bar graph depicting the average percent area occupied by CGRP-positive neurons within Rexeds laminae I–IV. There were no significant differences (ANOVA, $P > 0.05$) in the percent area occupied by CGRP-positive fibres between the treatment groups. (**e**) Withdrawal reflex in response to a hot light spot directed to the plantar surface of the hind paw. The reflex time is similar in all the groups (ANOVA, $P > 0.05$). Data are presented as means ± SEM; Scale bar: 100 μm (**a–d**). Regenerative sprouting and long distance regeneration of the transected corticospinal tract (CST). Transected CST axons do not sprout in (**g**) control IgG treated, non-trained or (**h**) IgG treated, trained animals. Rostral to the lesion sprouting fibres were found in (**i**) 11C7 treated, non-trained as well as (**j**) 11C7 treated, trained animals. (**k**) Fibres grow towards the caudal spinal cord (2 mm) and (**l**) arborize in response to Nogo-A antibody treatment (5 mm, representative picture for Nogo-A antibody treated, trained animal). (**m**) regeneration was increased in Nogo-A antibody treated animals independent of locomotor training. (ANOVA, Bonferroni *post hoc*, 11C7/trained $P \leqslant 0.01$). Data are presented as means ± SEM; $*P \leqslant 0.05$; $**P \leqslant 0.01$; Arrowheads: Regenerating CST fibre; Scale bar: 100 μm (**a–d**), 50 μm (**e** and **f**).

influence or interfere with the sprouting response after 11C7 antibody treatment.

Quantification of 5-HT positive varicosities on motoneuron cell bodies

Bouton-like varicosities of 5-HT immunoreactive fibres were present throughout laminae VII and IX in all four groups. Serotonergic innervation of motoneurons was quantified as previously described (Mullner *et al*., 2008), based on the assumption that these close appositions correspond to serotonergic synapses on motoneurons (Alvarez *et al*., 1998). Non-trained IgG rats showed very few boutons per 1000 μm^2 soma surface (Fig. 6f) with a small increase after locomotor training (Fig. 6g). In 11C7 treated animals a significant increase in labelled boutons was observed in non-trained (Fig. 6h and j; $P = 0.006$) and trained animals (Fig. 6i and j; $P = 0.009$).

Taken together, anti-Nogo-A antibody treatment but not training alone led to a significant increase in serotonergic innervation of motoneurons. Training did not interfere with the increased synaptic reinnervation of motoneurons in animals receiving locomotor training in combination with anti-Nogo-A antibody treatment.

Discussion

Two different patterns of hindlimb movements as observed during bipedal stepping on the treadmill developed in spinal cord injured rats under the influence of either anti-Nogo-A antibody treatment or, alternatively, daily treadmill exercise. Rats treated with anti-Nogo-A antibody alone developed a consistent, well coordinated step cycle with greater than a normal step height and short swing duration. This movement strategy led to good coordination

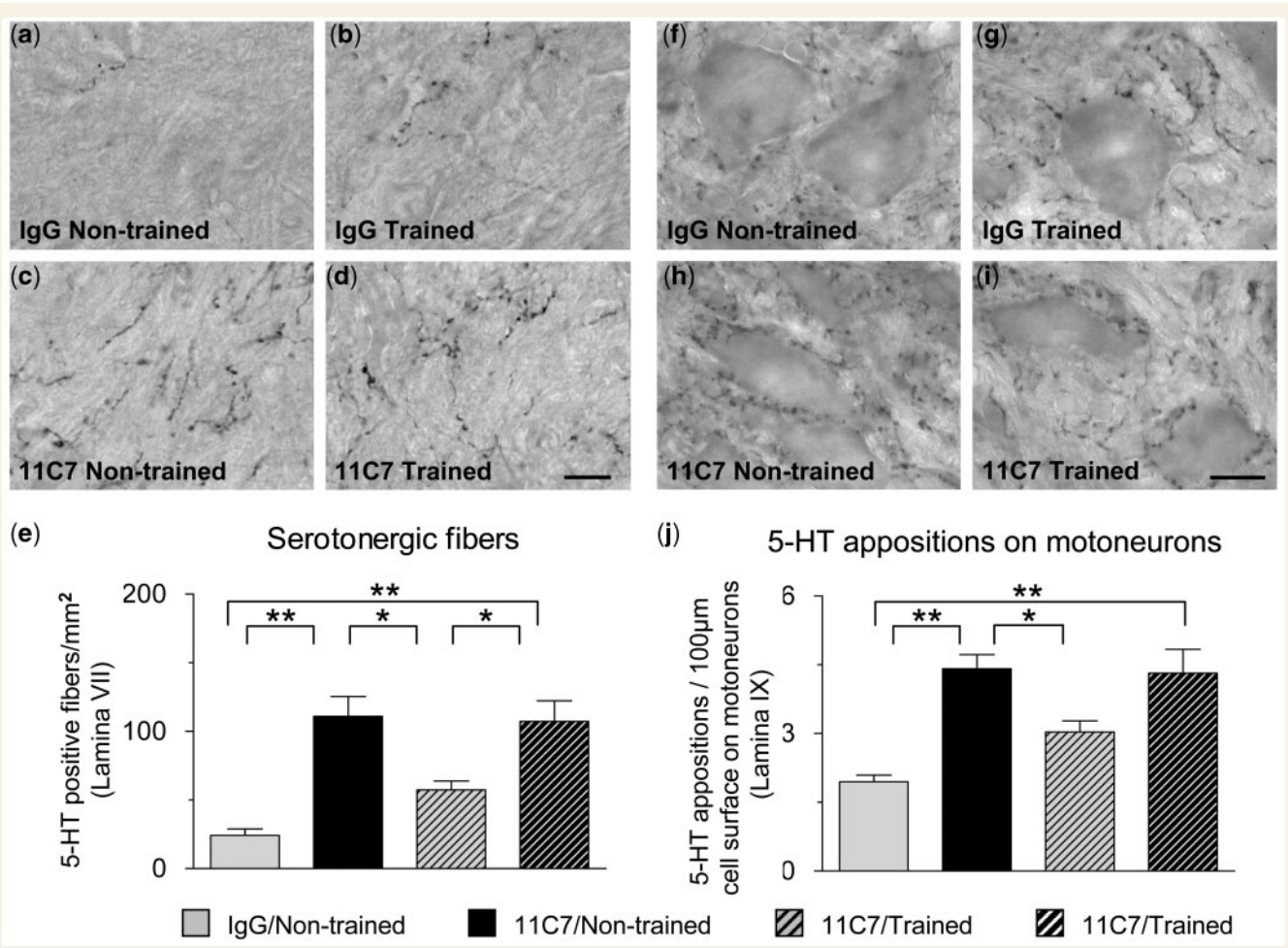

Figure 6 Recovery of serotonergic innervation after anti-Nogo-A antibody treatment or/and training. Few 5HT-positive fibres were found in Rexed's layer VII of (**a**) IgG treated, non-trained as well as (**b**) IgG treated, trained animals but significantly more in (**c**) 11C7 treated, non-trained and (**d**) 11C7 treated, trained rats. (**e**) Bar graph depicting that Nogo-A antibody treatment significantly increased the density of 5HT positive neurons in the caudal spinal cord independent of locomotor training (ANOVA, Bonferroni *post hoc*, $P \leqslant 0.05$). The number of 5-HT positive, bouton-like appositions on motoneurons (Rexed's lamina IV) was very low in (**f**) IgG treated, non-trained as well as (**g**) IgG treated, trained animals but significantly increased in (**h**) 11C7 treated, non-trained and (**i**) 11C7 treated, trained animals (ANOVA, Bonferroni *post hoc*, $P \leqslant 0.05$). (**j**) The number of presumptive serotonergic synaptic terminals on motoneurons relative to motoneuron circumference are shown for four treatment groups. Data are presented as means ± SEM; $*P \leqslant 0.05$; Scale bar: 50 µm.

between distal joints and prevented paw dragging, which typically occurred in the control IgG treated, non-trained animals. On the other hand, 40 min of daily treadmill training over 8 weeks resulted in well coordinated, long but low, sweeping steps with pronounced toe dragging. In line with the different movement patterns obtained in the two different treatment groups, the rats with combined simultaneous antibody treatment and forced exercise on the treadmill did not show an additive or enhanced but rather a diminished functional recovery effect, suggesting interference of both movement strategies and their underlying mechanisms.

It is important to note that our incomplete lesions allowed the rats to spontaneously recover a certain degree of hindlimb use; therefore, non-trained rats developed locomotor capacity probably by 'self-training' in their cages. The treadmill trained rats were forced to step both bipedally and quadrupedally daily on treadmill belts, in addition to their regular cage activity.

The effect of anti-Nogo-A antibody treatment

Anti-Nogo-A antibody treatment, together with the spontaneous 'training' of the animals in their cages, resulted in a high degree of functional restoration of hindlimb locomotion in line with earlier observations (Merkler *et al*., 2001; Liebscher *et al*., 2005). The hyperflexion of the knee could possibly compensate for the drop foot, a typical feature in incomplete spinal cord injured rats and humans. In addition, anti-Nogo-A antibody treatment resulted in highly consistent step shapes and step cycles, and little variability in interlimb coordination and joint

angle shapes, which resembled the value of non-disabled rats more closely. Anatomically, we observed CST fibre regeneration in anti-Nogo-A treated animals. CST fibres were able to circumvent the lesion and extended their axons into the denervated caudal spinal cord as previously reported (Liebscher *et al*., 2005; Freund *et al*., 2006). In parallel, we found an increase in 5-HT positive fibres in these animals, which resulted in the restoration of the original 5-HT fibre density and motoneuron innervation in the lumbar spinal cord (Mullner *et al*., 2008). These anatomical results suggest that anti-Nogo-A antibody-induced regeneration and sprouting of descending systems contribute to the observed changes in locomotor function. The beneficial effects of elevated serotonin levels in the lumbar spinal cord after spinal cord injury have been shown in earlier transplantation studies (Ribotta *et al*., 2000).

The effect of bipedal and quadrupedal treadmill training

Intense locomotor training on the motorized treadmill resulted in significant modifications of specific kinematic parameters of stepping which were, however, different from those seen in intact or lesioned control IgG treated as well as anti-Nogo-A antibody treated animals. Trained rats had a significantly lower step height with longer swing duration, and significant alterations in hip and ankle joint movements. These long, low, sweeping steps seemed well adapted to the biomechanical constraints imposed by the lesion and to the fast locomotion imposed by the treadmill. We did not observe an increase in CST or 5HT fibre regeneration or sprouting at the lumbar level of the spinal cord in trained animals in accordance with previous observations (Engesser-Cesar *et al*., 2007).

Treadmill trained, completely transected mice, rats, cats and humans can improve assisted stepping capacity. This is correlated with decreased inhibition in the lumbar cord (de Leon *et al*., 1999; Tillakaratne *et al*., 2002), changes in electrophysiological characteristics of motoneurons (Petruska *et al*., 2007), as well as an increased expression of neurotrophic factors (Gomez-Pinilla *et al*., 2002; Boyce *et al*., 2007). The repeated activation by sensory afferents of specific spinal networks probably facilitates locomotor circuit and motoneuron activation in these trained subjects. Such changes may also account for the functional adaptations observed in the present study in incomplete spinal cord lesioned rats.

After incomplete lesions, spontaneous stepping ability largely depends on the amount of remaining descending control (Schucht *et al*., 2002; Reinkensmeyer *et al*., 2006). The effect of treadmill training after incomplete injury has been under debate until now, probably mainly due to the difficulty of separating spontaneous 'self-training' effects from specific therapy-induced effects (Fouad *et al*., 2000; Thota *et al*., 2001; Multon *et al*., 2003). Here, by the combination of bipedal and quadrupedal stepping on a fast running treadmill, the development of a specific stepping pattern in response to training could be clearly shown.

Even though Nogo-A antibody treatment or locomotor training resulted in significantly different movement strategies on the treadmill, both interventions independently led to better performance of the lesioned rats on the inclined grid walk, a novel motor task, to which the rats had not been exposed before.

The effect of combinatorial treatment

The observation that the simultaneous application of locomotor training and anti-Nogo-A antibodies led to interference and poorer locomotor performance suggests that the mechanisms underlying the development of the two treatment-specific movement patterns are not only different but possibly competitive. Antibody treatment increased regrowth and sprouting of descending fibre tracts as exemplified by CST or 5-HT fibres; such fibres could re-establish pre-lesion connections. Intraspinal circuits may then adapt to this reinnervation leading to the observed behaviourally meaningful hindlimb movement pattern. On the other hand, in the animals that received intense locomotor training afferent inputs might have 'replaced' the lost descending pathways (Petruska *et al*., 2007), leading to spinal circuits that mostly rely on afferent inputs.

Plastic changes after injuries have not only been correlated with recovery of function and locomotion, but also with neurogenic pain and autonomic dysreflexia (Christensen and Hulsebosch, 1997*a*; Ackery *et al*., 2007). CGRP is a neuropeptide found in nociceptive unmyelinated (C) and thinly myelinated (A) afferent fibres projecting primarily to lamina I and II of the dorsal horn (Hokfelt *et al*., 1992). After spinal cord injury CGRP upregulation as well as sprouting of CGRP positive fibres has been reported (Christensen and Hulsebosch, 1997*b*). Pain could interfere with locomotor training or spinal learning (Ferguson *et al*., 2006; Petruska *et al*., 2007). Following neutralization of Nogo-A or the Nogo-A receptor NgR after spinal cord injury an increase in pain perception has never been observed (Thallmair *et al*., 1998; Liebscher *et al*., 2005; Freund *et al*., 2006) and there was no aberrant sprouting of nociceptive fibres into deeper laminae of the dorsal horn (Cafferty and Strittmatter, 2006). We tested for changes in pain withdrawal reflex in response to noxious heat stimuli in the rats with combined anti-Nogo-A antibody treatment and locomotor training. Withdrawal responses were equal in all treatment groups and were not altered in comparison to uninjured rats (Liebscher *et al*., 2005). In animals that received the combined treatment, CGRP fibres did not show abnormal innervation patterns. Thus, enhanced neurogenic pain or aberrant sprouting of CGRP could not explain the behavioural results we observed after the combined treatment group.

Training of one particular task can interfere with performance in another task (Bigbee *et al*., 2007; Girgis *et al*., 2007) suggesting that, in the present case, two different conditions and learning strategies—'self training' in the cage versus forced treadmill training—may have interfered with each other, thus leading to a suboptimal behavioural outcome. Preliminary results indicate that such interference did not occur when treadmill training was started 2 weeks after the end of the antibody application (unpublished results). The optimal arrangement of combinatorial treatments e.g. a growth and regeneration enhancing treatment followed by the appropriate rehabilitative training remains an exciting challenge for future studies.

Our data suggests that the behavioural effects and the underlying plasticity mechanisms induced by task specific treadmill training or spontaneous recovery after anti-Nogo-A antibody treatment are different. A mechanistic understanding of the effect of each treatment as well as their potential interactions will be crucial to design optimal treatment protocols for experimental and future human therapies.

Supplementary material

Supplementary material is available at *Brain* online.

Funding

Christopher and Dana Reeve Foundation International Scientific Consortium for SCI (Springfield, NJ); National Center of Competence in Research 'Neural Plasticity and Repair' of the Swiss National Science Foundation.

References

Ackery AD, Norenberg MD, Krassioukov A. Calcitonin gene-related peptide immunoreactivity in chronic human spinal cord injury. Spinal Cord 2007; 45: 678–86.

Alvarez FJ, Pearson JC, Harrington D, Dewey D, Torbeck L, Fyffe RE. Distribution of 5-hydroxytryptamine-immunoreactive boutons on alpha-motoneurons in the lumbar spinal cord of adult cats. J Comp Neurol 1998; 393: 69–83.

Barbeau H, Rossignol S. Recovery of locomotion after chronic spinalization in the adult cat. Brain Res 1987; 412: 84–95.

Barriere G, Leblond H, Provencher J, Rossignol S. Prominent role of the spinal central pattern generator in the recovery of locomotion after partial spinal cord injuries. J Neurosci 2008; 28: 3976–87.

Basso DM, Beattie MS, Bresnahan JC. A sensitive and reliable locomotor rating scale for open field testing in rats. J Neurotrauma 1995; 12: 1–21.

Bigbee AJ, Crown ED, Ferguson AR, Roy RR, Tillakaratne NJ, Grau JW, et al. Two chronic motor training paradigms differentially influence acute instrumental learning in spinally transected rats. Behav Brain Res 2007; 180: 95–101.

Boyce VS, Tumolo M, Fischer I, Murray M, Lemay MA. Neurotrophic factors promote and enhance locomotor recovery in untrained spinalized cats. J Neurophysiol 2007; 98: 1988–96.

Cafferty WB, Strittmatter SM. The Nogo-Nogo receptor pathway limits a spectrum of adult CNS axonal growth. J Neurosci 2006; 26: 12242–50.

Christensen MD, Hulsebosch CE. Chronic central pain after spinal cord injury. J Neurotrauma 1997a; 14: 517–37.

Christensen MD, Hulsebosch CE. Spinal cord injury and anti-NGF treatment results in changes in CGRP density and distribution in the dorsal horn in the rat. Exp Neurol 1997b; 147: 463–75.

Courtine G, Roy RR, Hodgson J, McKay H, Raven J, Zhong H, et al. Kinematic and EMG determinants in quadrupedal locomotion of a non-human primate (Rhesus). J Neurophysiol 2005; 93: 3127–45.

Courtine G, Schieppati M. Tuning of a basic coordination pattern constructs straight-ahead and curved walking in humans. J Neurophysiol 2004; 91: 1524–35.

Courtine G, Song B, Roy RR, Zhong H, Herrmann JE, Ao Y, et al. Recovery of supraspinal control of stepping via indirect propriospinal relay connections after spinal cord injury. Nat Med 2008; 14: 69–74.

de Leon RD, Hodgson JA, Roy RR, Edgerton VR. Full weight-bearing hindlimb standing following stand training in the adult spinal cat. J Neurophysiol 1998; 80: 83–91.

de Leon RD, Tamaki H, Hodgson JA, Roy RR, Edgerton VR. Hindlimb locomotor and postural training modulates glycinergic inhibition in the spinal cord of the adult spinal cat. J Neurophysiol 1999; 82: 359–69.

Dietz V, Harkema SJ. Locomotor activity in spinal cord-injured persons. J Appl Physiol 2004; 96: 1954–60.

Edgerton VR, Leon RD, Harkema SJ, Hodgson JA, London N, Reinkensmeyer DJ, et al. Retraining the injured spinal cord. J Physiol 2001; 533 (Pt 1): 15–22.

Edgerton VR, Tillakaratne NJ, Bigbee AJ, de Leon RD, Roy RR. Plasticity of the spinal neural circuitry after injury. Ann Rev Neurosci 2004; 27: 145–67.

Ferguson AR, Crown ED, Grau JW. Nociceptive plasticity inhibits adaptive learning in the spinal cord. Neuroscience 2006; 141: 421–31.

Fong AJ, Cai LL, Otoshi CK, Reinkensmeyer DJ, Burdick JW, Roy RR, et al. Spinal cord-transected mice learn to step in response to quipazine treatment and robotic training. J Neurosci 2005; 25: 11738–47.

Fouad K, Metz GA, Merkler D, Dietz V, Schwab ME. Treadmill training in incomplete spinal cord injured rats. Behav Brain Res 2000; 115: 107–13.

Freund P, Schmidlin E, Wannier T, Bloch J, Mir A, Schwab ME, et al. Nogo-A-specific antibody treatment enhances sprouting and functional recovery after cervical lesion in adult primates. Nat Med 2006; 12: 790–2.

Girgis J, Merrett D, Kirkland S, Metz GA, Verge V, Fouad K. Reaching training in rats with spinal cord injury promotes plasticity and task specific recovery. Brain 2007; 130 (Pt 11): 2993–3003.

Gomez-Pinilla F, Ying Z, Roy RR, Molteni R, Edgerton VR. Voluntary exercise induces a BDNF-mediated mechanism that promotes neuroplasticity. J Neurophysiol 2002; 88: 2187–95.

Harel NY, Strittmatter SM. Can regenerating axons recapitulate developmental guidance during recovery from spinal cord injury? Nat Rev Neurosci 2006; 7: 603–16.

Hargreaves K, Dubner R, Brown F, Flores C, Joris J. A new and sensitive method for measuring thermal nociception in cutaneous hyperalgesia. Pain 1988; 32: 77–88.

Herzog A, Brosamle C. 'Semifree-floating' treatment: a simple and fast method to process consecutive sections for immunohistochemistry and neuronal tracing. J Neurosci Methods 1997; 72: 57–63.

Hokfelt T, Arvidsson U, Ceccatelli S, Cortes R, Cullheim S, Dagerlind A, et al. Calcitonin gene-related peptide in the brain, spinal cord, and some peripheral systems. Ann N Y Acad Sci 1992; 657: 119–34.

Ichiyama RM, Courtine G, Gerasimenko YP, Yang GJ, van den Brand R, Lavrov IA, et al. Step training reinforces specific spinal locomotor circuitry in adult spinal rats. J Neurosci 2008; 28: 7370–5.

Ichiyama RM, Gerasimenko YP, Zhong H, Roy RR, Edgerton VR. Hindlimb stepping movements in complete spinal rats induced by epidural spinal cord stimulation. Neurosci Lett 2005; 383: 339–44.

Kubasak MD, Jindrich DL, Zhong H, Takeoka A, McFarland KC, Munoz-Quiles C, et al. OEG implantation and step training enhance hindlimb-stepping ability in adult spinal transected rats. Brain 2008; 131 (Pt 1): 264–76.

Liebscher T, Schnell L, Schnell D, Scholl J, Schneider R, Gullo M, et al. Nogo-A antibody improves regeneration and locomotion of spinal cord-injured rats. Ann Neurol 2005; 58: 706–19.

Merkler D, Metz GA, Raineteau O, Dietz V, Schwab ME, Fouad K. Locomotor recovery in spinal cord-injured rats treated with an antibody neutralizing the myelin-associated neurite growth inhibitor Nogo-A. J Neurosci 2001; 21: 3665–73.

Mullner A, Gonzenbach RR, Weinmann O, Schnell L, Liebscher T, Schwab ME. Lamina-specific restoration of serotonergic projections

after Nogo-A antibody treatment of spinal cord injury in rats. Eur J Neurosci 2008; 27: 326–33.

Multon S, Franzen R, Poirrier AL, Scholtes F, Schoenen J. The effect of treadmill training on motor recovery after a partial spinal cord compression-injury in the adult rat. J Neurotrauma 2003; 20: 699–706.

Oertle T, van der Haar ME, Bandtlow CE, Robeva A, Burfeind P, Buss A, et al. Nogo-A inhibits neurite outgrowth and cell spreading with three discrete regions. J Neurosci 2003; 23: 5393–406.

Ondarza AB, Ye Z, Hulsebosch CE. Direct evidence of primary afferent sprouting in distant segments following spinal cord injury in the rat: colocalization of GAP-43 and CGRP. Exp Neurol 2003; 184: 373–80.

Petruska JC, Ichiyama RM, Jindrich DL, Crown ED, Tansey KE, Roy RR, et al. Changes in motoneuron properties and synaptic inputs related to step training after spinal cord transection in rats. J Neurosci 2007; 27: 4460–71.

Raineteau O, Fouad K, Noth P, Thallmair M, Schwab ME. Functional switch between motor tracts in the presence of the mAb IN-1 in the adult rat. Proc Natl Acad Sci USA 2001; 98: 6929–34.

Reinkensmeyer DJ, Aoyagi D, Emken JL, Galvez JA, Ichinose W, Kerdanyan G, et al. Tools for understanding and optimizing robotic gait training. J Rehabil Res Dev 2006; 43: 657–70.

Ribotta MG, Provencher J, Feraboli-Lohnherr D, Rossignol S, Privat A, Orsal D. Activation of locomotion in adult chronic spinal rats is achieved by transplantation of embryonic raphe cells reinnervating a precise lumbar level. J Neurosci 2000; 20: 5144–52.

Rossignol S, Drew T, Brustein E, Jiang W. Locomotor performance and adaptation after partial or complete spinal cord lesions in the cat. Prog Brain Res 1999; 123: 349–65.

Schucht P, Raineteau O, Schwab ME, Fouad K. Anatomical correlates of locomotor recovery following dorsal and ventral lesions of the rat spinal cord. Exp Neurol 2002; 176: 143–53.

Schwab ME. Nogo and axon regeneration. Curr Opin Neurobiol 2004; 14: 118–24.

Thallmair M, Metz GA, Z'Graggen WJ, Raineteau O, Kartje GL, Schwab ME. Neurite growth inhibitors restrict plasticity and functional recovery following corticospinal tract lesions. Nat Neurosci 1998; 1: 124–31.

Thota A, Carlson S, Jung R. Recovery of locomotor function after treadmill training of incomplete spinal cord injured rats. Biomed Sci Instrum 2001; 37: 63–7.

Tillakaratne NJ, de Leon RD, Hoang TX, Roy RR, Edgerton VR, Tobin AJ. Use-dependent modulation of inhibitory capacity in the feline lumbar spinal cord. J Neurosci 2002; 22: 3130–43.

Timoszyk WK, Nessler JA, Acosta C, Roy RR, Edgerton VR, Reinkensmeyer DJ, et al. Hindlimb loading determines stepping quantity and quality following spinal cord transection. Brain Res 2005; 1050: 180–9.

Weinmann O, Schnell L, Ghosh A, Montani L, Wiessner C, Wannier T, et al. Intrathecally infused antibodies against Nogo-A penetrate the CNS and downregulate the endogenous neurite growth inhibitor Nogo-A. Mol Cell Neurosci 2006; 32: 161–73.